

Novel Dissimilar Joints between 2.25Cr-1Mo Steel and Alloy 800H through Additive Manufacturing

J. S. Zuback, T. Mukherjee, T. A. Palmer and T. DebRoy

Graduate Student

Pennsylvania State University

November 18th, 2016

AWS FABTECH Conference, Las Vegas, NV

Financial support: U.S. Department of Energy grant number DE-NE0008280

Collaborators: Dr. W. Zhang, Ohio State University, Dr. Z. Feng, Oak Ridge National Laboratory

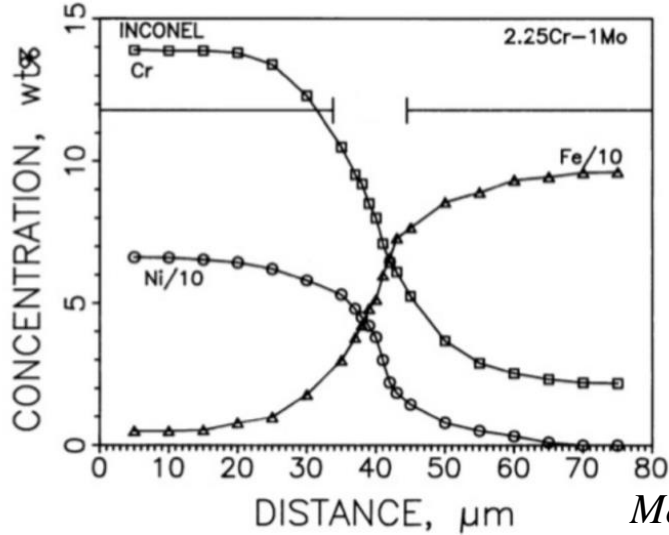
Advisor: S. A. David, Oak Ridge National Laboratory

TPOC: Dr. S. Sham, U.S. Department of Energy



Ferritic (2.25Cr-1Mo Steel) to austenitic (800H) joints

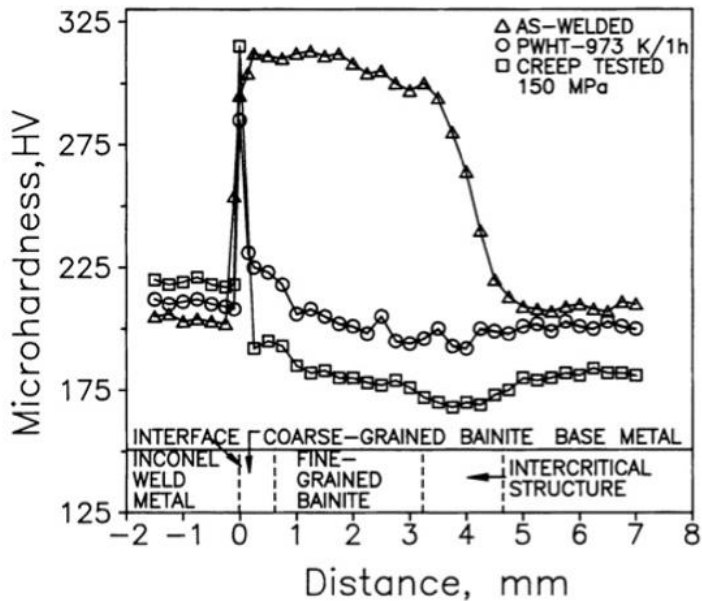
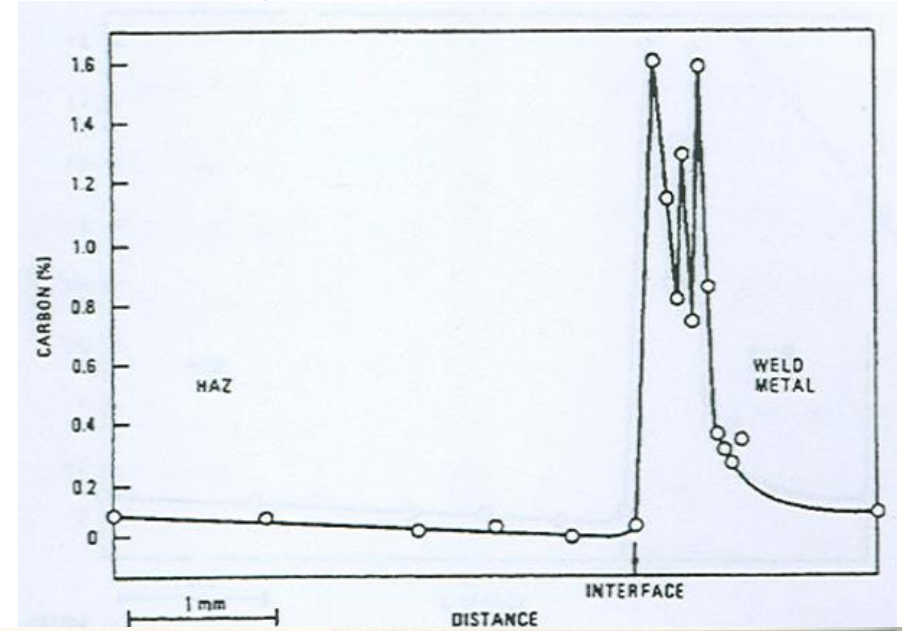
Sharp changes in composition and micro-hardness



Laha
Metall. Mater. Trans A
2001

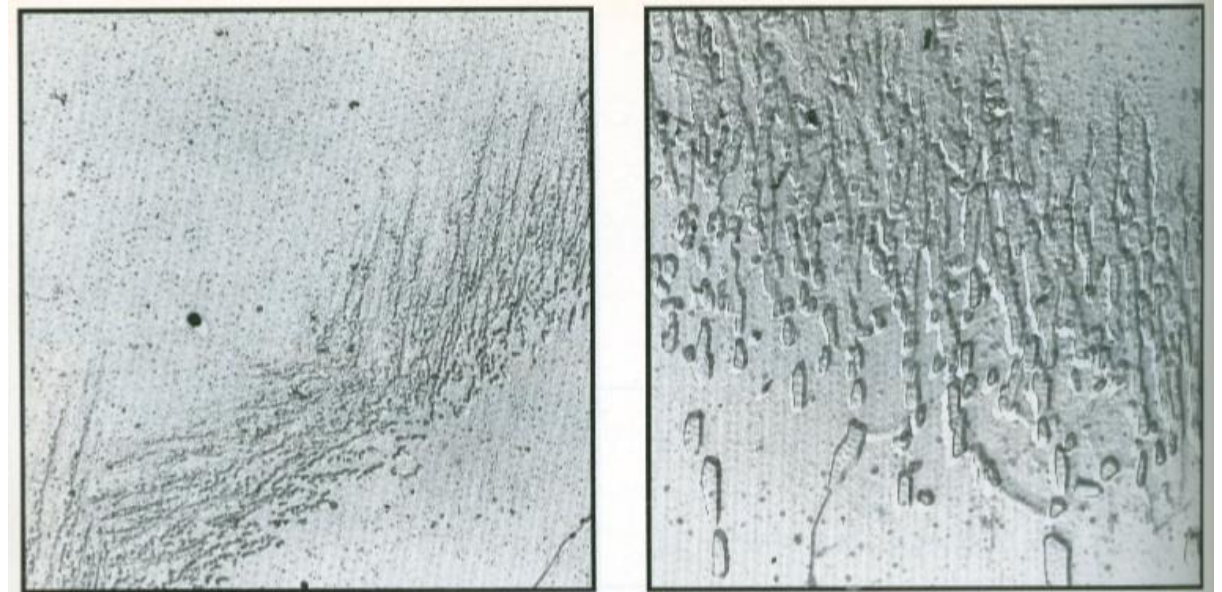
Carbon diffusion
towards austenitic alloy

Ryder
*Trends in Electric Utility
Research, 1984*



Carbide formation
along HAZ of
ferritic steel

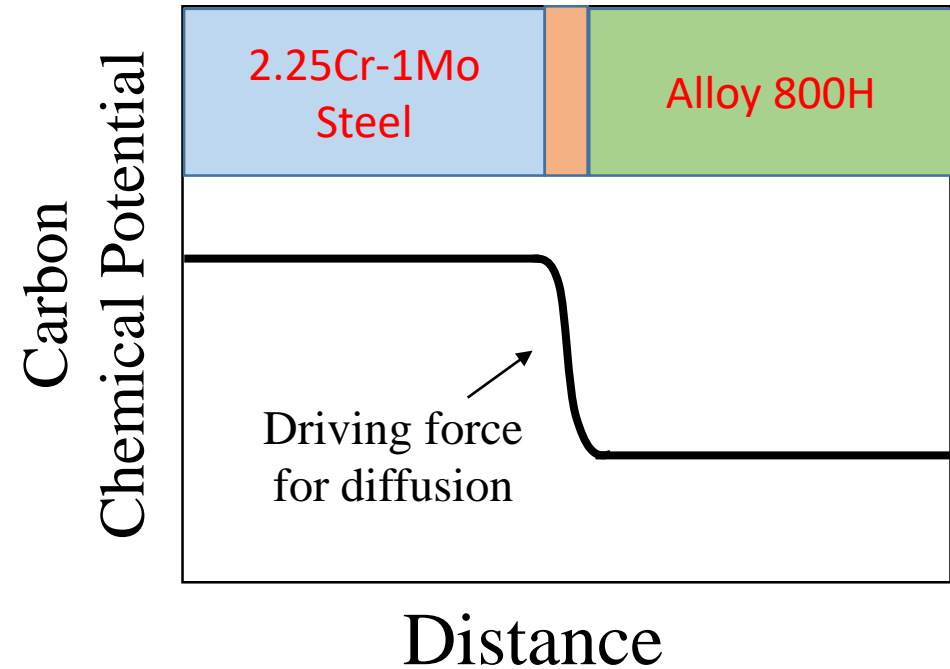
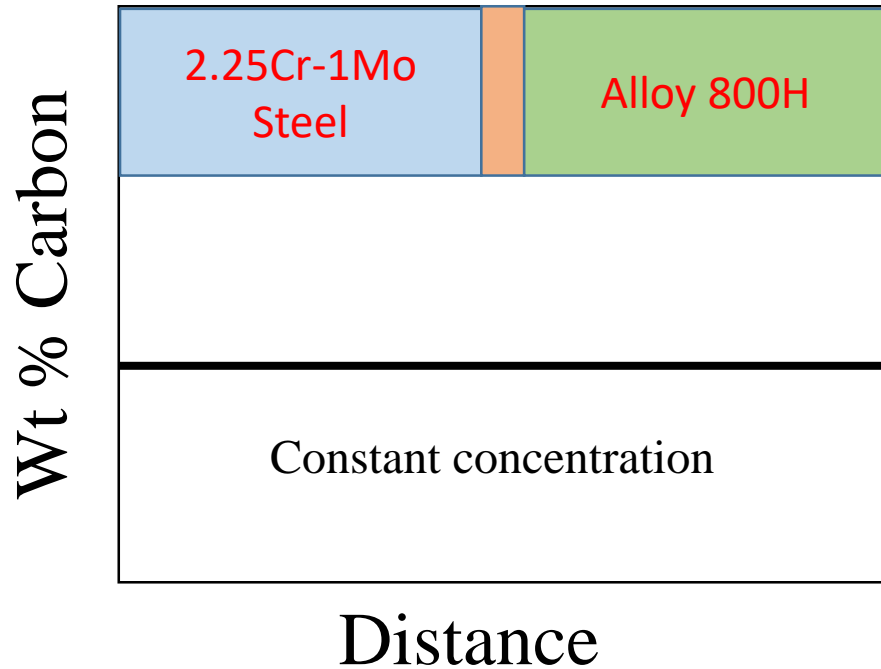
Gittos
Welding Journal
1992



What causes carbon diffusion?

Carbon chemical potential gradient

- Diffusion flux is typically governed by the concentration gradient in many applications
- Here, the system needs to be define in terms of the chemical potential gradient



Fick's first law of diffusion

$$J_i = -D_i \frac{dc_i}{dx}$$



$$J_i = -\frac{L_i}{T} \frac{d\mu_i}{dx}$$

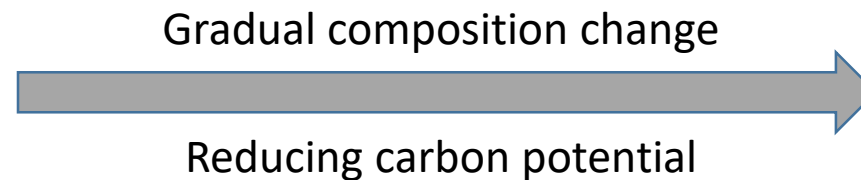
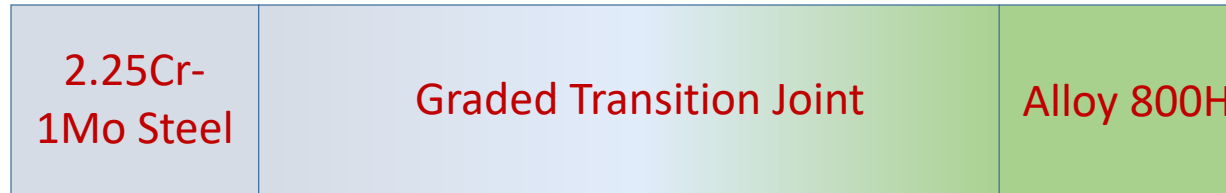
Depends on alloying elements



Reduce carbon diffusion by minimizing carbon potential gradient

- (a) Thermodynamically model carbon potential gradient for various compositionally graded transition joints
- (b) Fabricate selected transition joints by additive manufacturing
- (c) Test fabricated joints

2.25Cr-1Mo Steel	
Element	Wt%
C	0.1
Cr	2.25
Fe	Balance
Mo	1
Mn	0.5
Ni	0.045
Si	0.5



Alloy 800H	
Element	Wt%
Al	0.6
C	0.1
Cr	21
Cu	0.75
Fe	39.5
Mn	1.5
Ni	Balance
Si	1
Ti	0.6

Eliminates abrupt changes in mechanical properties, microstructure, and composition
 Reduces carbon potential gradient



How is chemical composition optimized?

1. Plot C-potential for a linear composition change and compare to minimized C-potential gradient

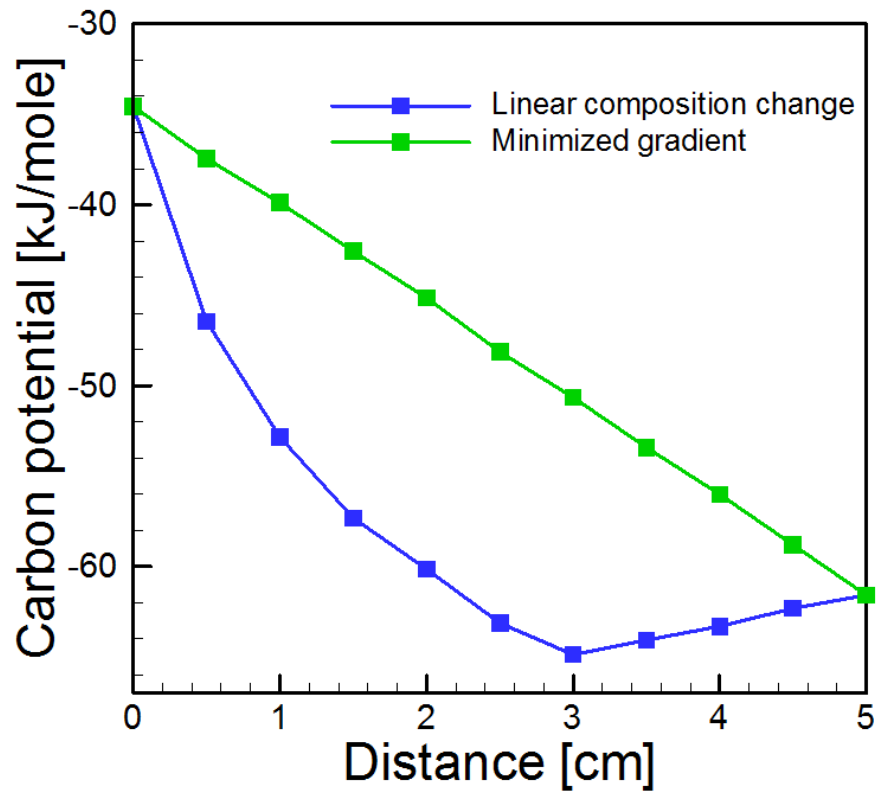
2. Calculate C-potential as a function of Cr concentration at all locations along transition joint

3. Use search algorithm for Cr concentration that gives target C-potential value

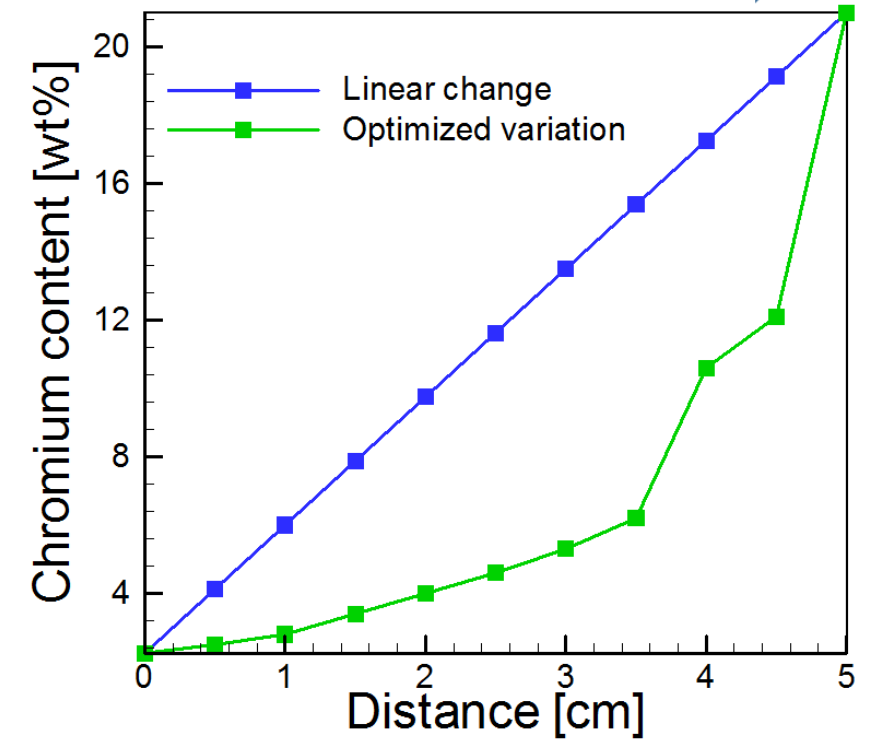
4. Repeat steps 1-3 for all locations. Output Cr concentration profile

5. Build transition joint with minimized C-potential gradient

2.25Cr-1Mo Steel → Alloy 800H



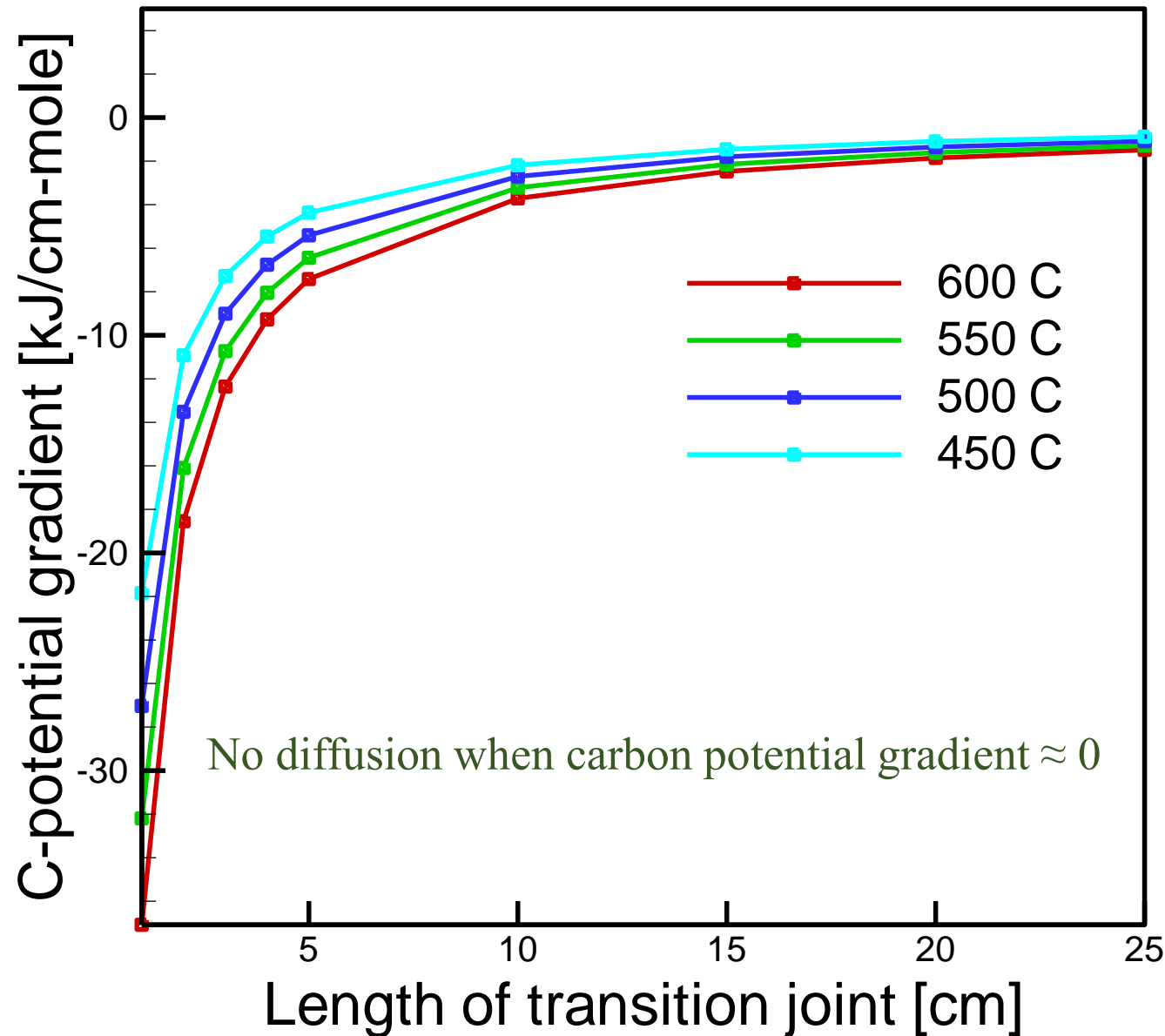
2.25Cr-1Mo Steel → Alloy 800H



2.25Cr-1Mo Steel



Alloy 800H



Carbon potential gradient = Driving force for carbon diffusion

At constant T, driving force depends on length

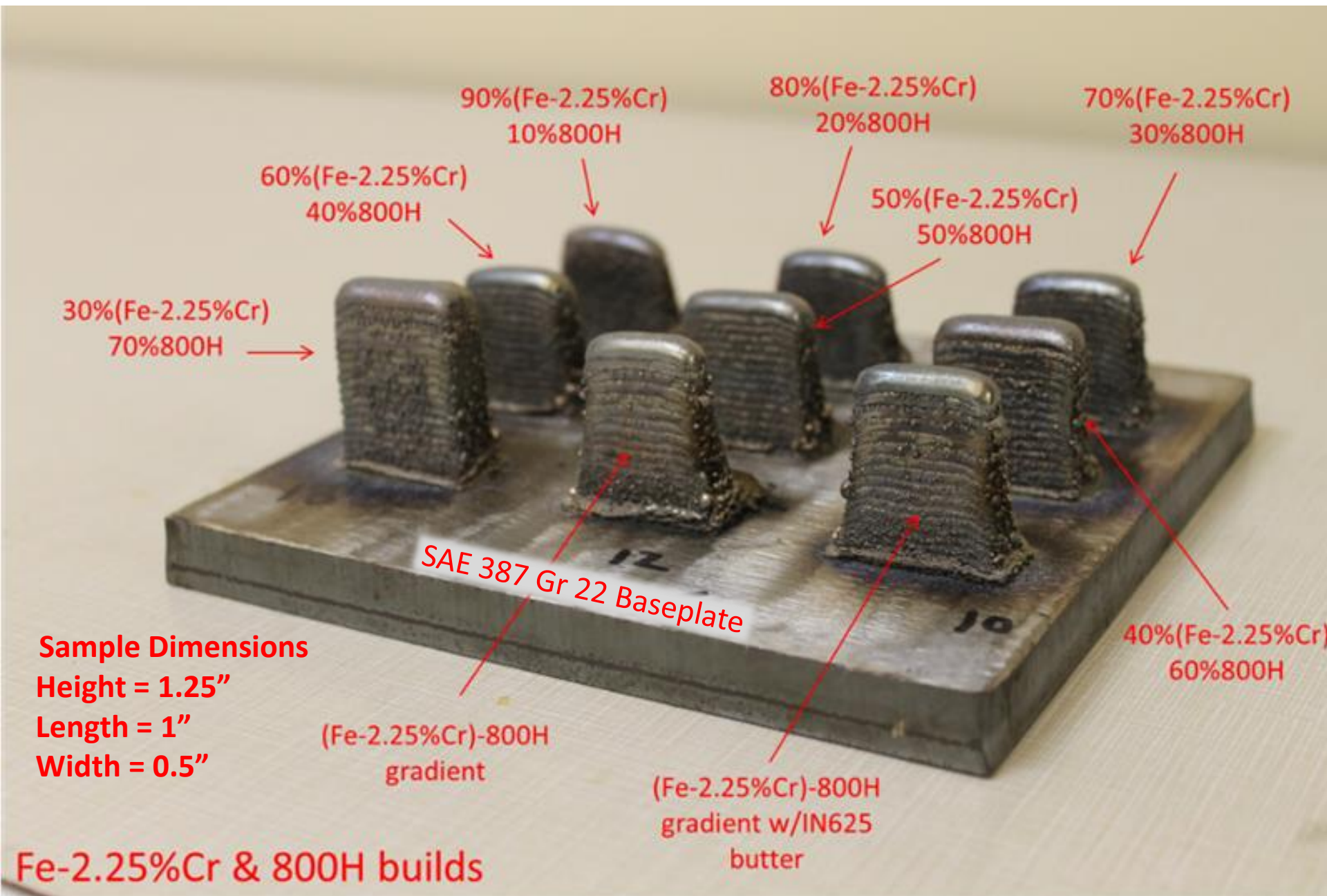
Assume an optimized change in C-potential from beginning to end of joint

Plot: Dependence of carbon potential gradient on length of transition joint for 4 temperatures

Finding:

- Marginal benefits for joints over 5 cm

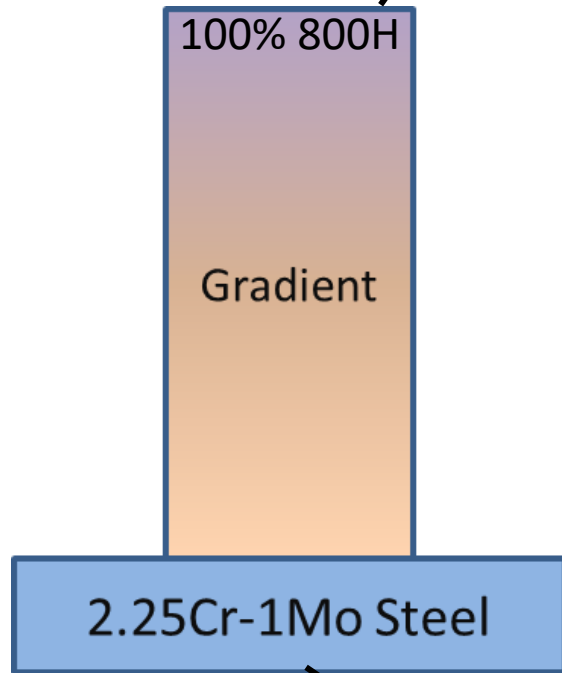
Fabrication of compositionally graded test specimens



Parameters	Values
Laser power (W)	2000
Beam radius (mm)	2.0
Scanning speed (mm/s)	10.6
Layer thickness (mm)	0.89
Substrate thickness (mm)	12.5

EPMA Results

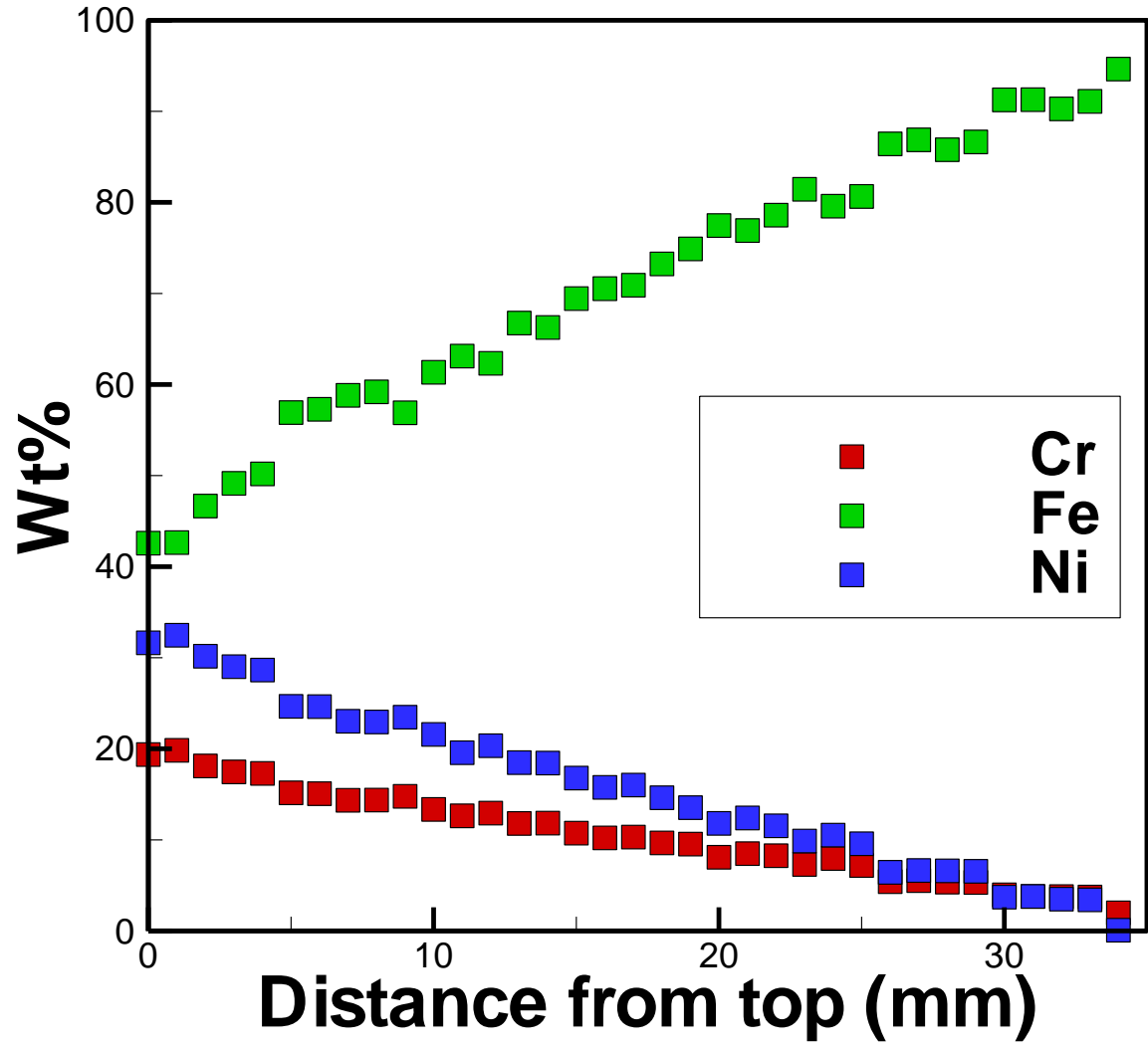
- 35 measurements
- 1 mm spacing
- From top (800H) into substrate (2.25Cr-1Mo steel)



Dist. from top [mm]	wt% C	wt% Si	wt% Cr	wt% Fe	wt% Mo	wt% Mn	wt% Ni	wt% Al
0	1.359	0.572	19.363	42.577	-	4.038	31.636	0.48
1	-	0.631	19.824	42.647	0.01	4.321	32.461	0.40
2	0.568	0.488	18.106	46.655	0.022	3.667	30.161	0.333
3	0.457	0.405	17.459	49.153	0.008	3.193	29.018	0.306
4	-	0.452	17.293	50.185	-	3.608	28.645	0.309
5	-	0.34	15.161	56.919	0.009	2.823	24.656	0.259
6	-	0.328	15.068	57.277	-	2.74	24.636	0.248
7	0.507	0.31	14.343	58.807	0.017	2.767	23.02	0.229
8	0.135	0.359	14.37	59.196	0.004	2.76	22.94	0.236
9	0.703	0.455	14.78	56.895	0.016	3.433	23.469	0.251
10	0.666	0.303	13.348	61.34	0.051	2.521	21.574	0.198
11	1.252	0.389	12.634	63.119	0.014	2.832	19.574	0.186

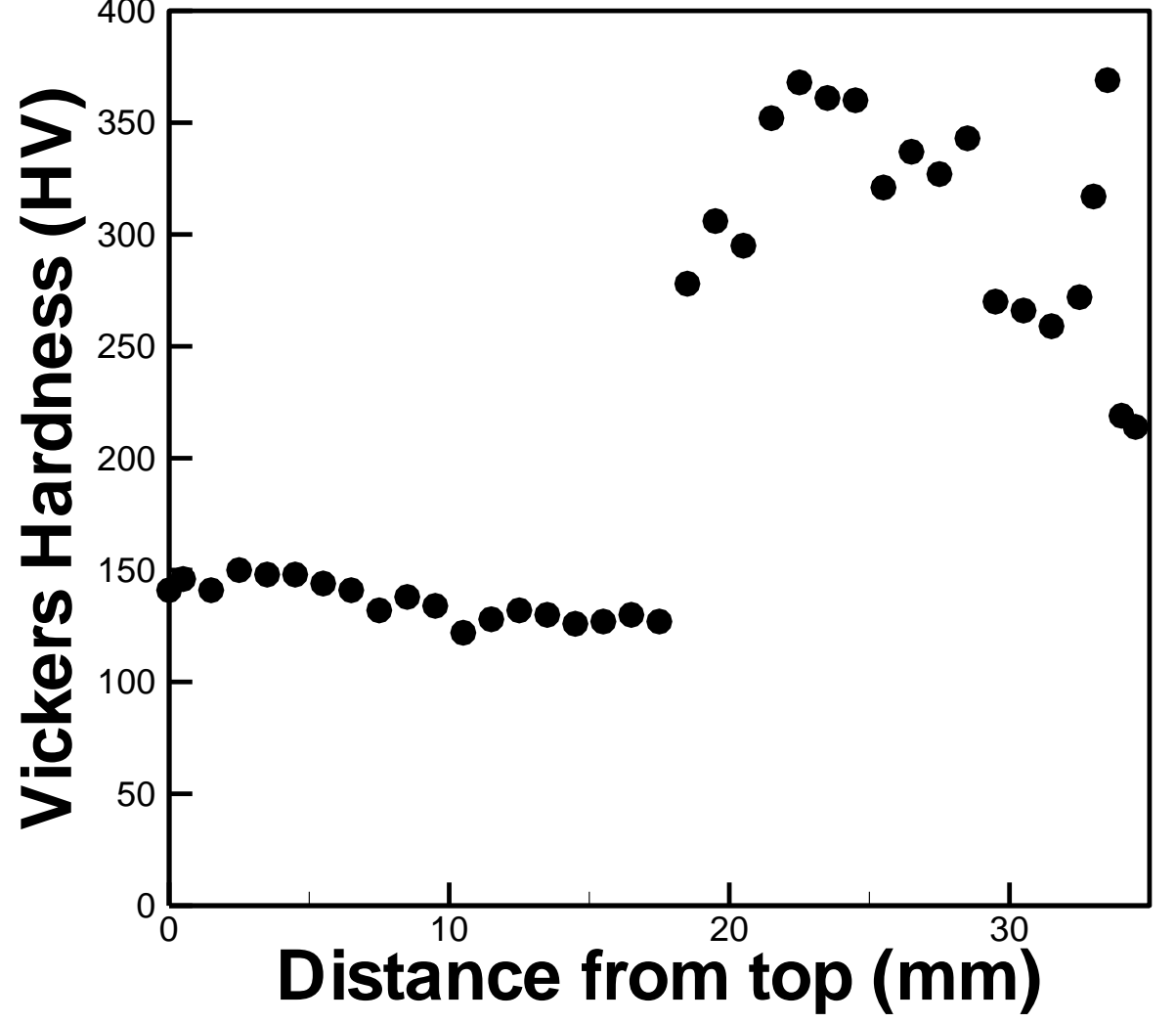
26	0.429	0.099	5.408	86.416	0.045	1.12	6.435	0.047
27	-	0.127	5.515	86.867	0.047	1.212	6.629	0.020
28	0.905	0.113	5.358	85.776	0.022	1.167	6.589	0.068
29	0.115	0.123	5.313	86.643	0.063	1.148	6.542	0.054
30	0.114	0.074	3.967	91.259	0.025	0.842	3.701	0.018
31	0.256	0.08	3.783	91.277	0.008	0.813	3.778	0.005
32	1.498	0.057	3.763	90.27	0.039	0.867	3.488	0.018
33	0.58	0.095	3.717	91.093	0.161	0.922	3.417	0.015
34	-	0.184	1.979	94.64	1.43	1.89	0.081	0.034

800H (Top)  Fe-2.25Cr (Bottom)

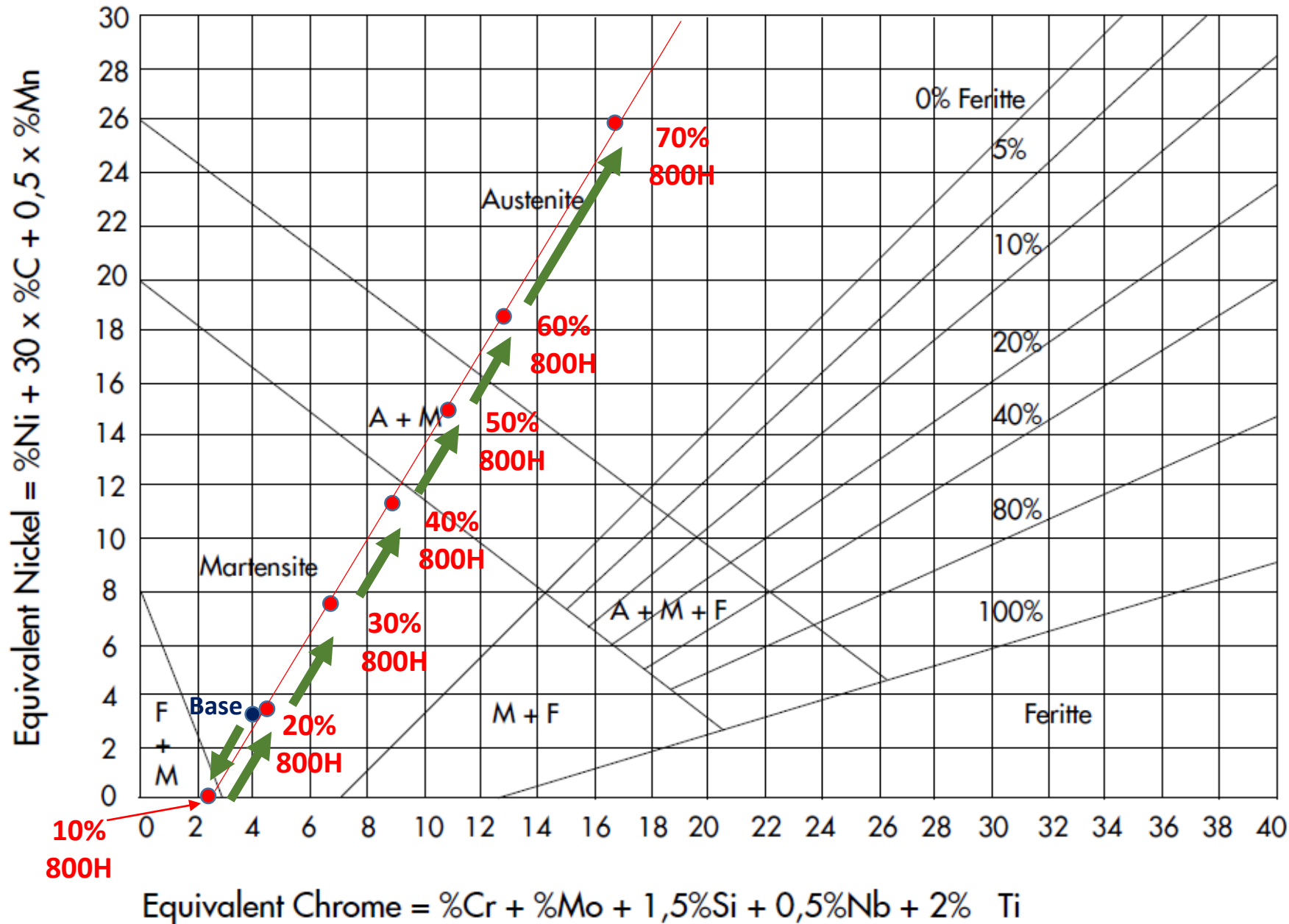


EPMA done at PSU MCL on CAMECA SXFive

800H (Top)  Fe-2.25Cr (Bottom)



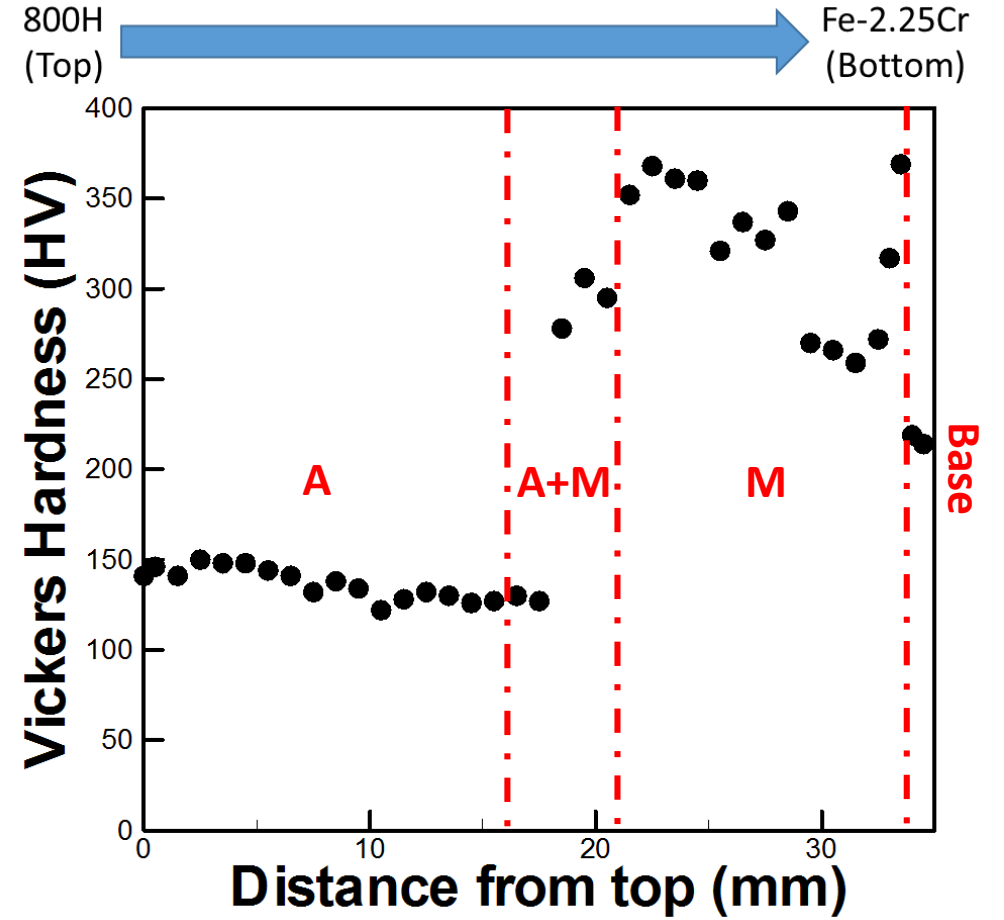
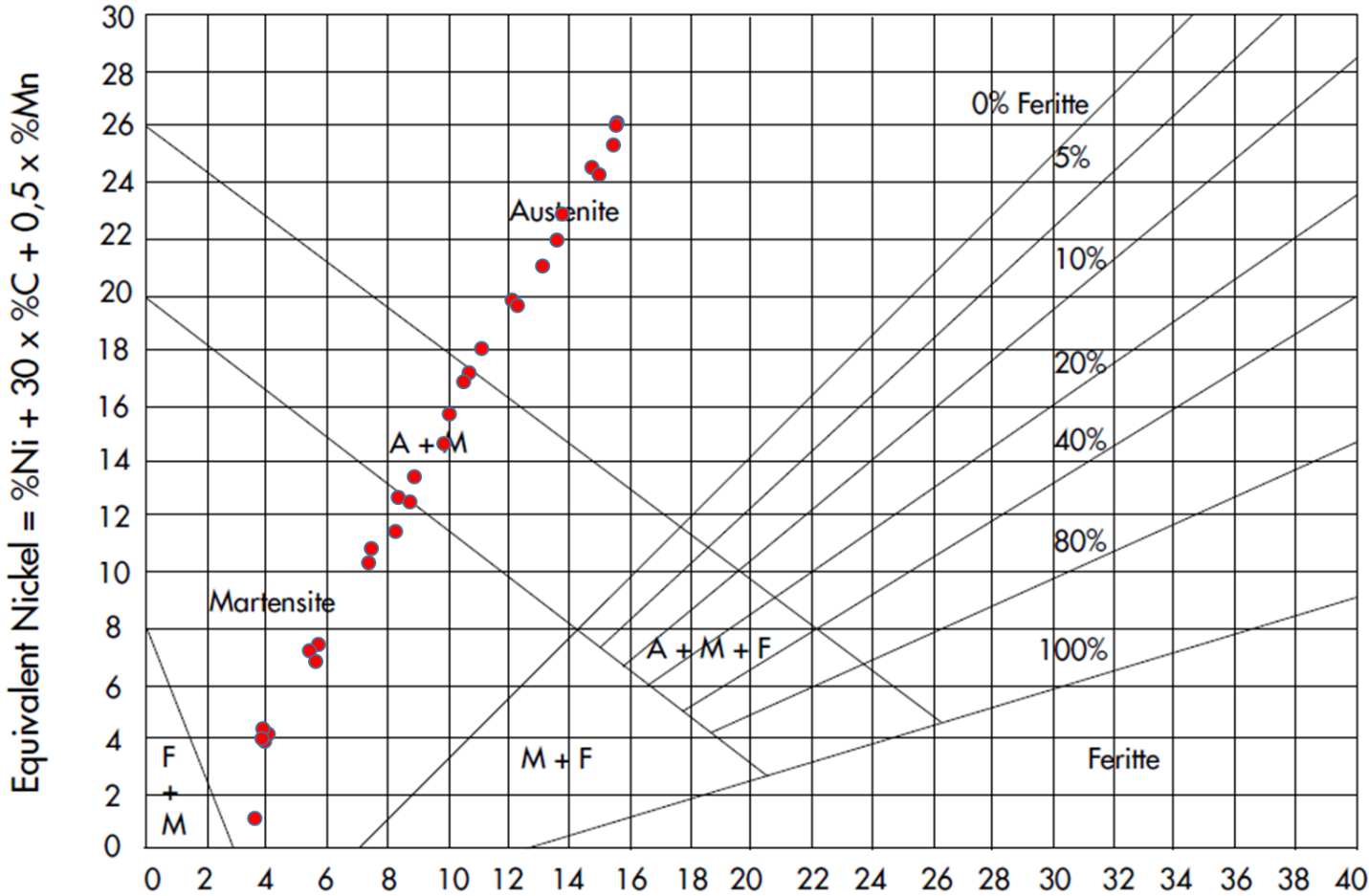
Hardness measurements taken on LECO M-400-G1 at PSU ARL (300g load)



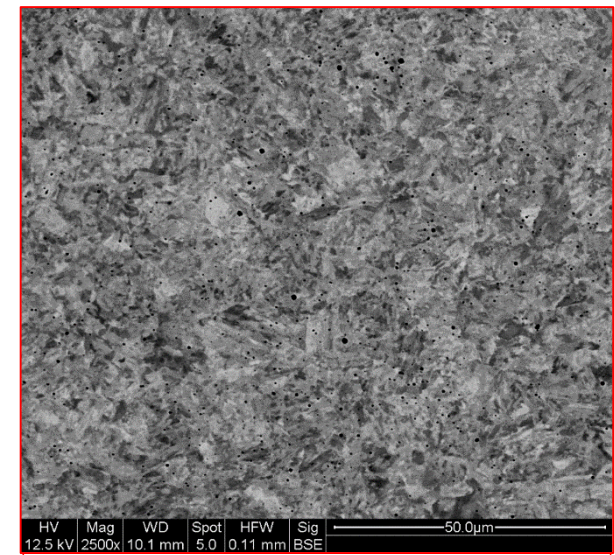
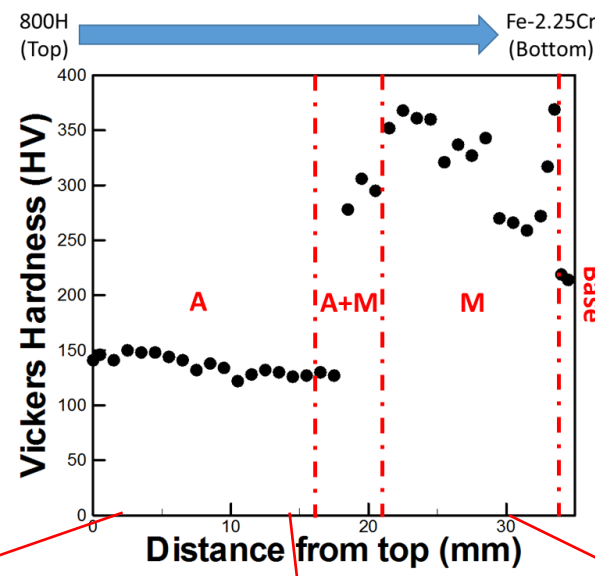
Schaeffler Constitution Diagram

- Commonly used when welding low alloy steels, austenitic stainless steels and dissimilar alloys
- Relates the composition to microstructure based on common cooling rates found in welding
- Here, it is used as a guide for predicting the microstructure in a low alloy steel to austenitic graded alloy

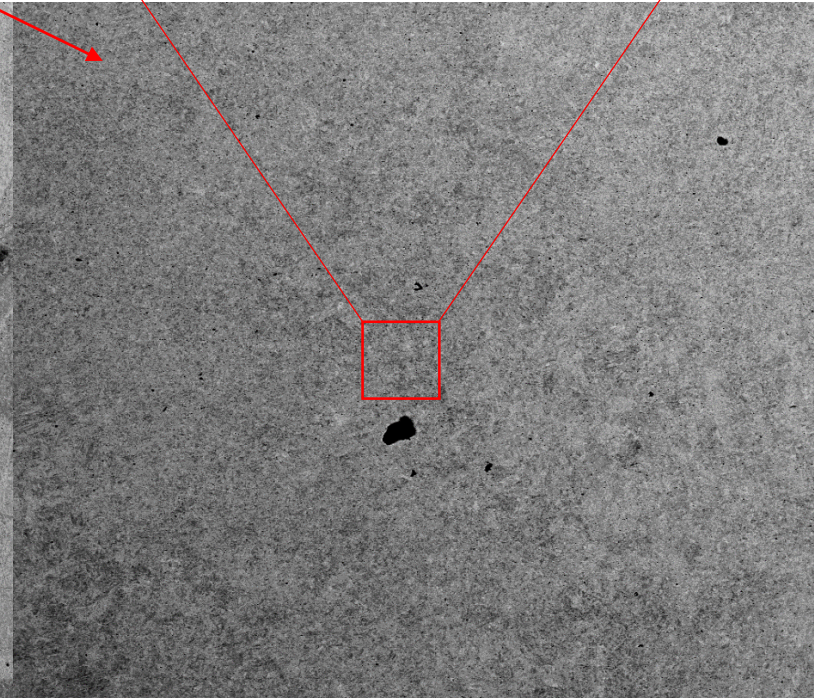
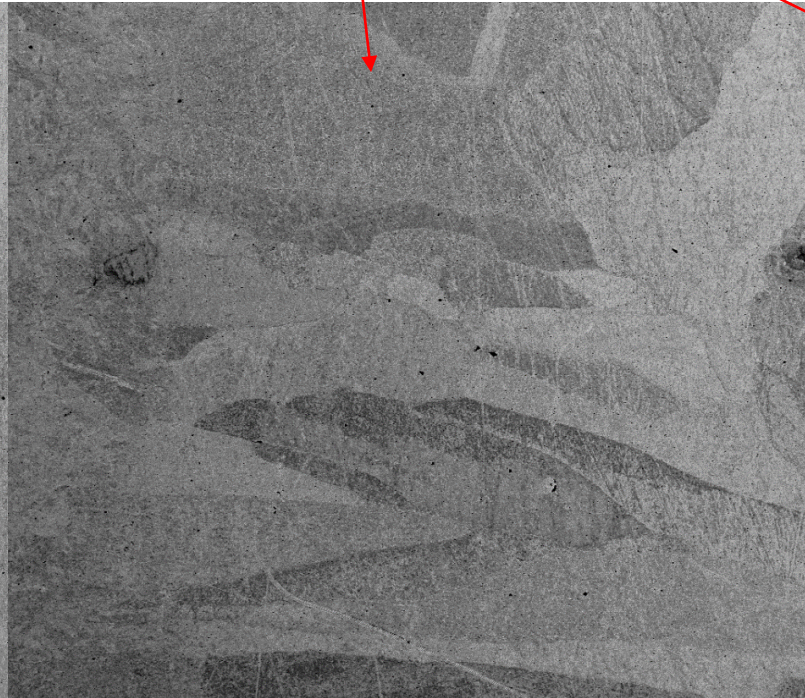
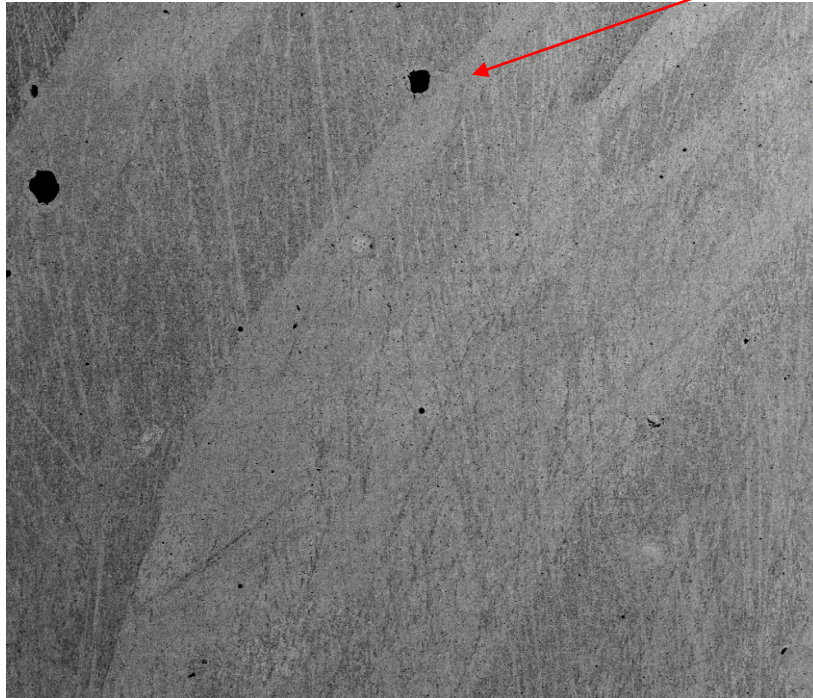
Changes in composition correspond to changes in microstructure



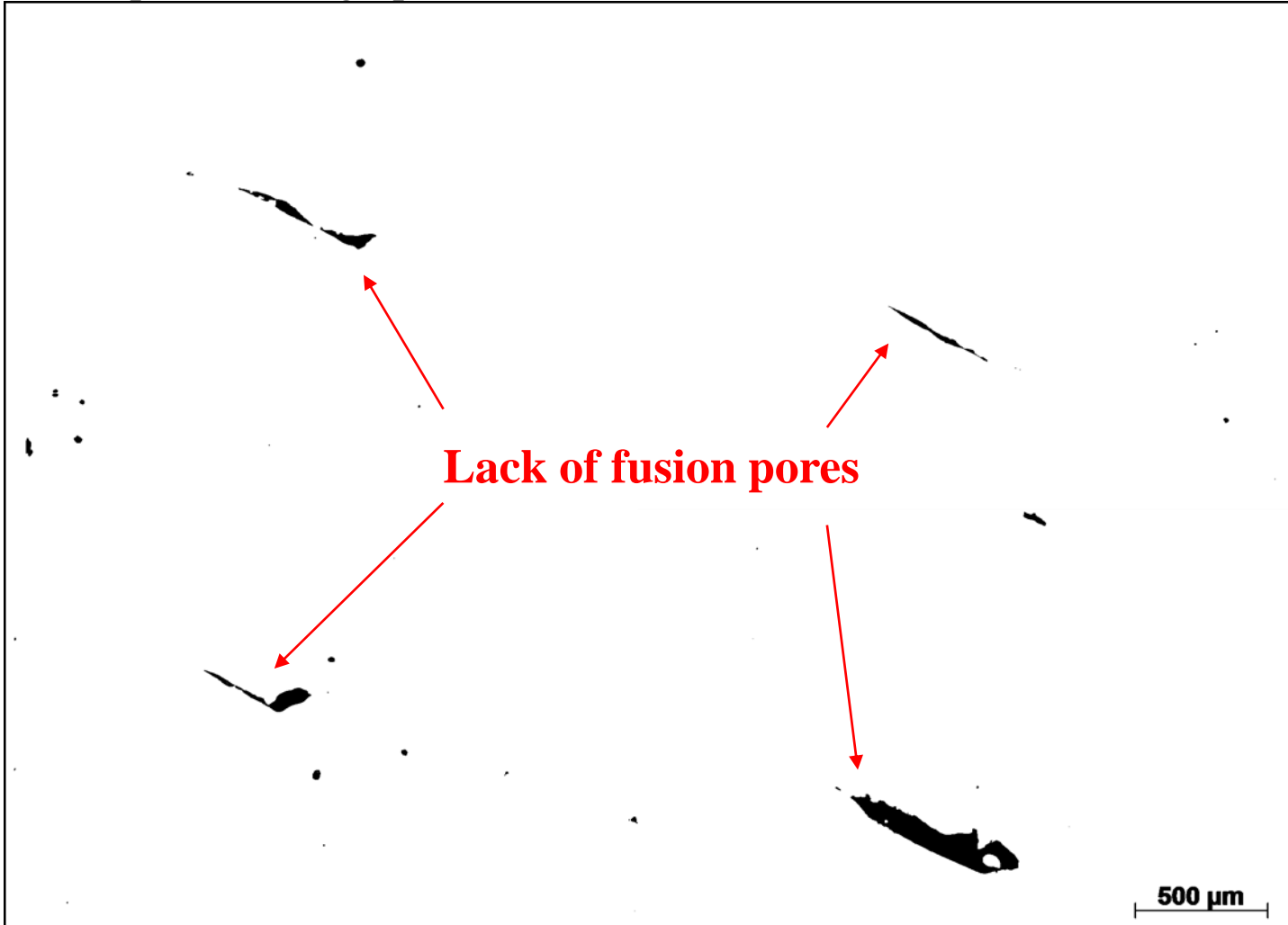
SEM Images



Noticeable change from very fine microstructural constituents to long, elongated columnar grains

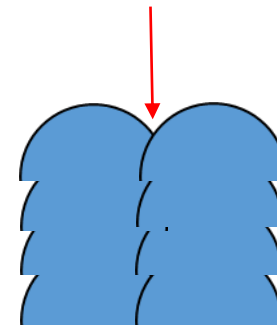


Optical micrograph shown in black and white scale for contrast



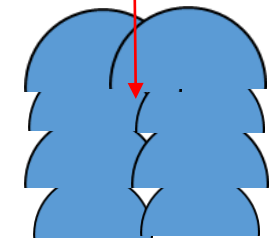
- Vertically aligned lack of fusion porosity caused by improper choice of hatch spacing
 - Only observed in layers close to baseplate
- Differences in melt pool dimensions

Proper bonding



Uniform melt pool

Improper bonding

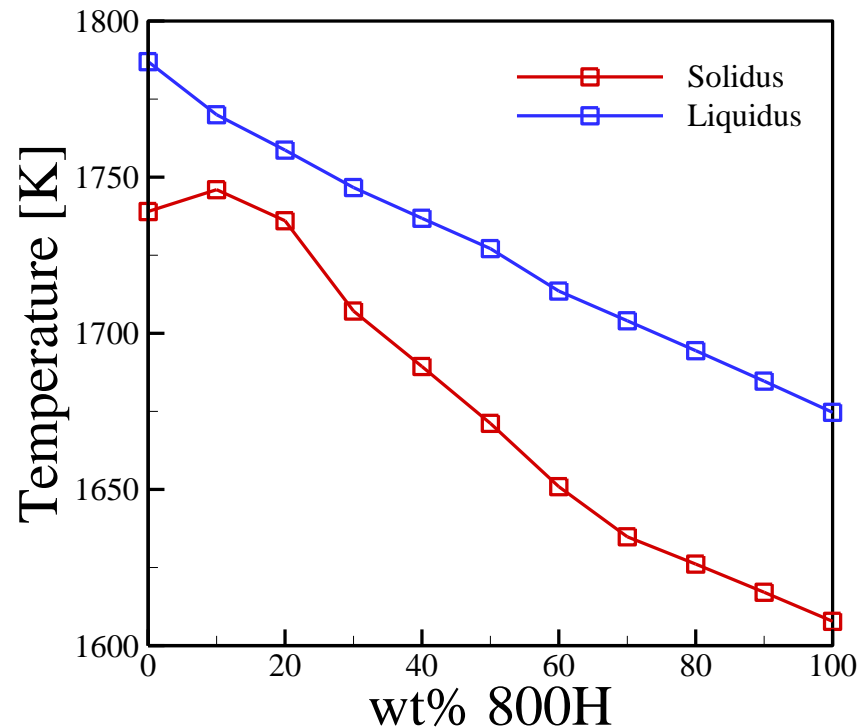


Non-uniform melt pool

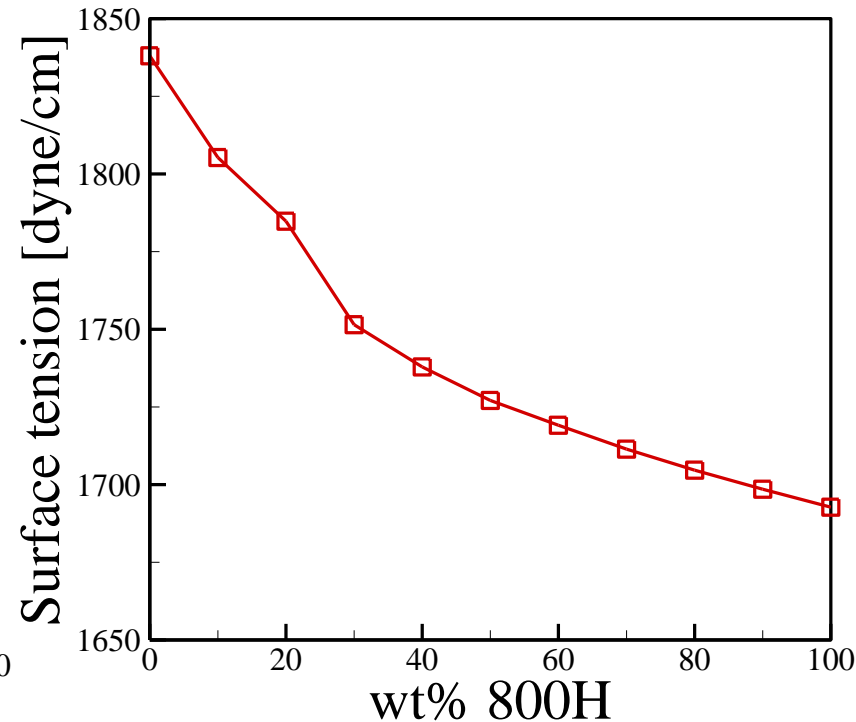
- Not all alloys are printed similarly due to differences in thermo-physical properties
- Leads to differences in molten pool geometry and susceptibility to defects

Notable differences in properties between 2.25Cr-1Mo Steel and Alloy 800H

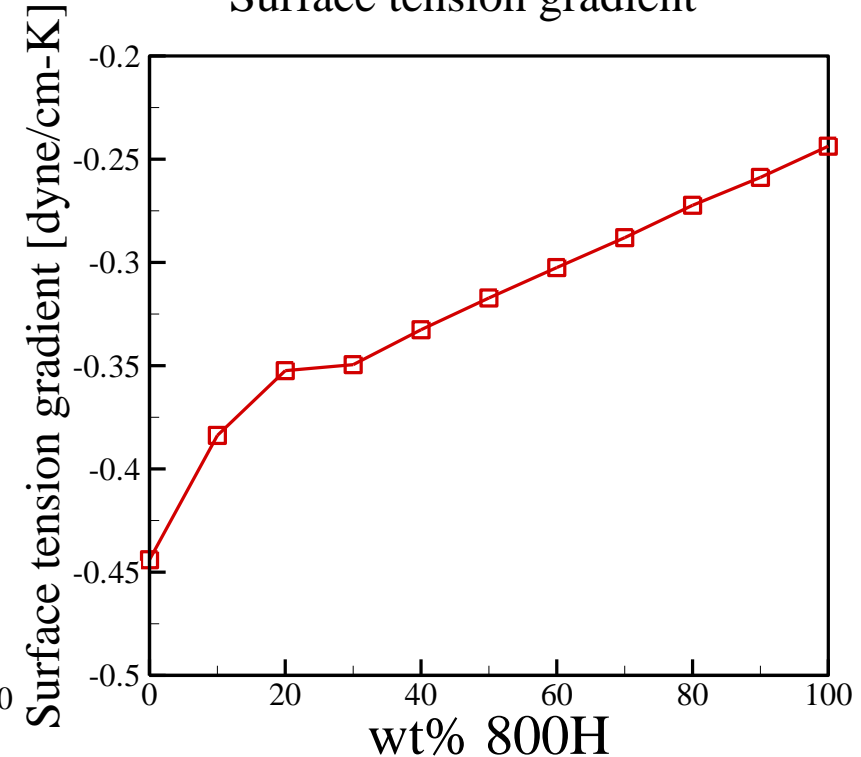
Solidus/Liquidus Temperature



Surface tension at liquidus temperature



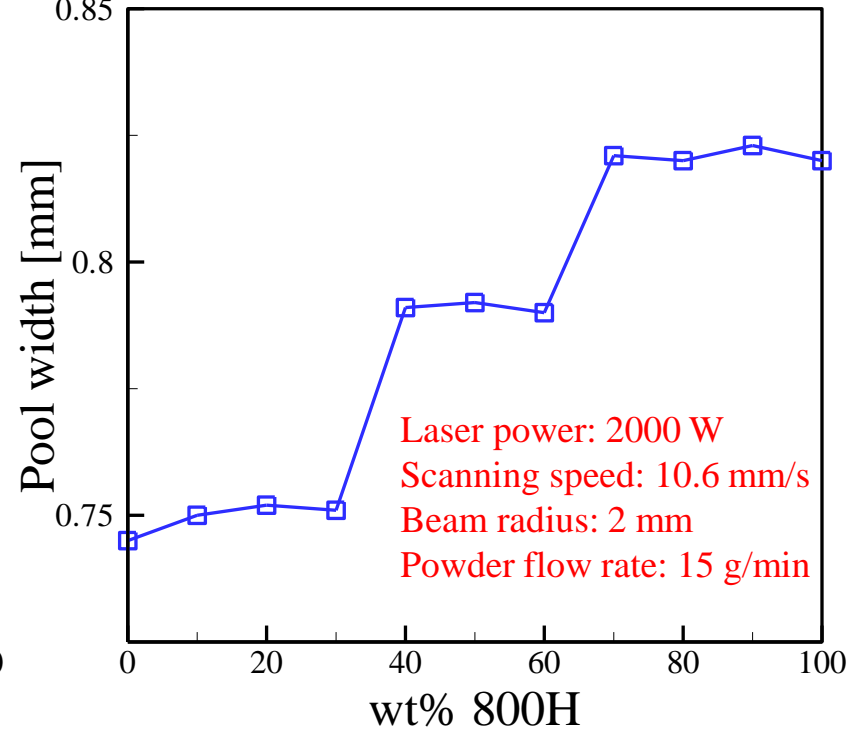
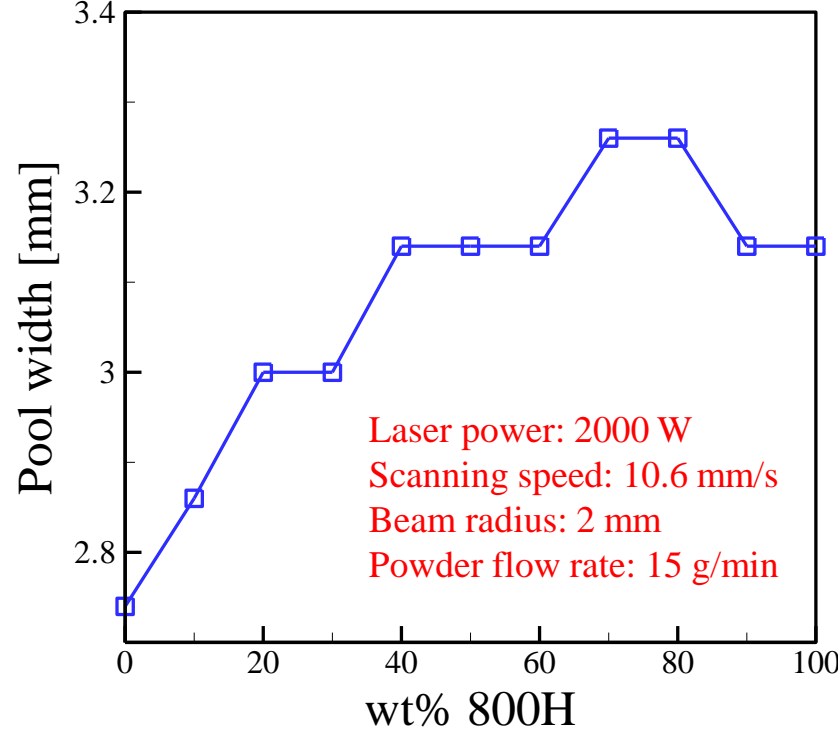
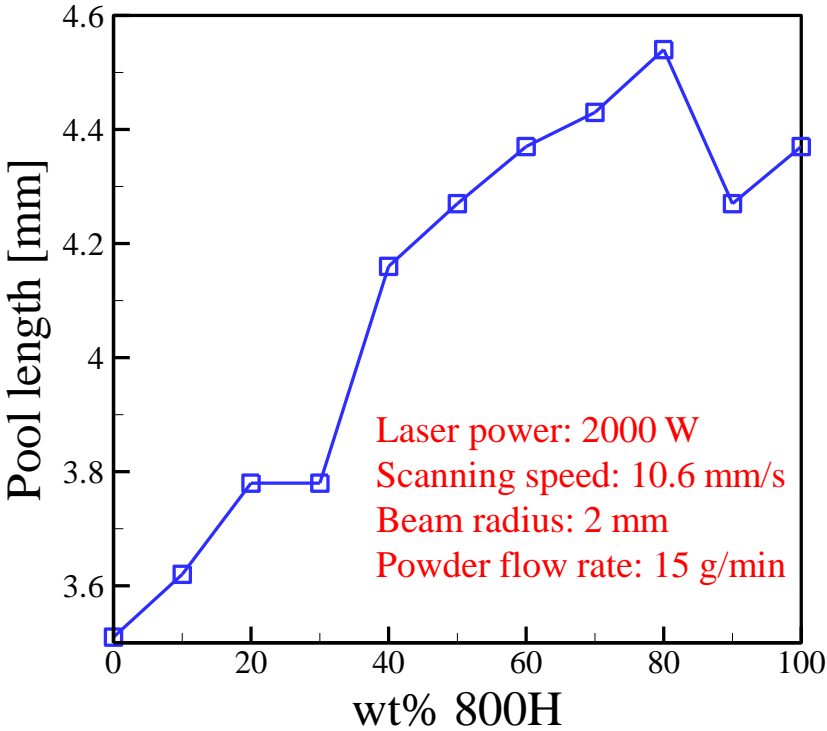
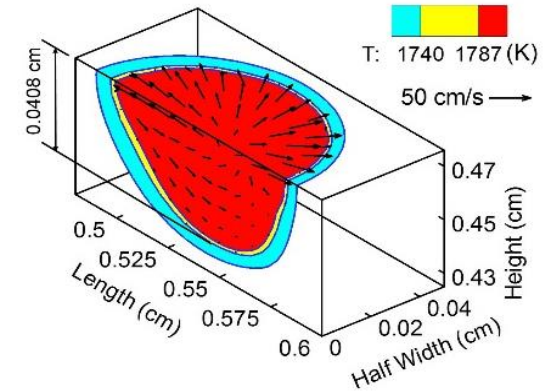
Surface tension gradient



Material properties
Process parameters
Surrounding conditions

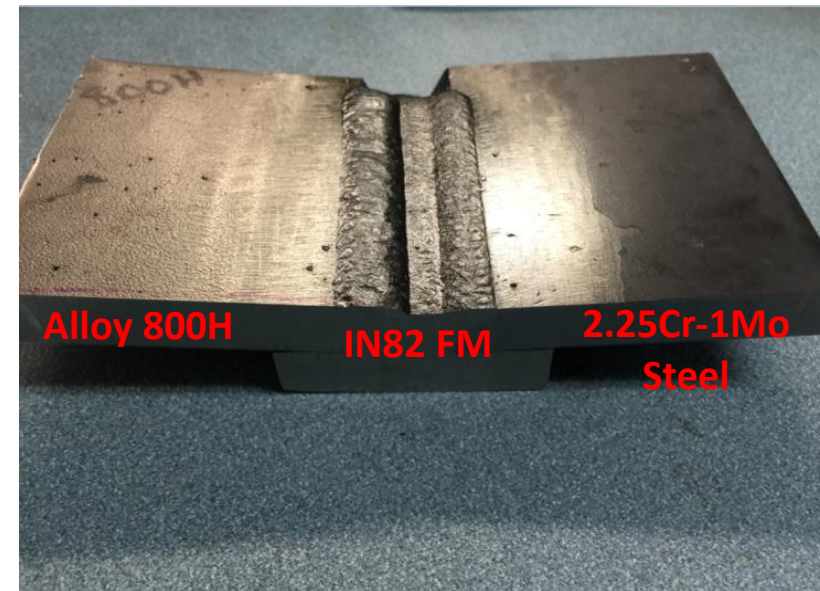
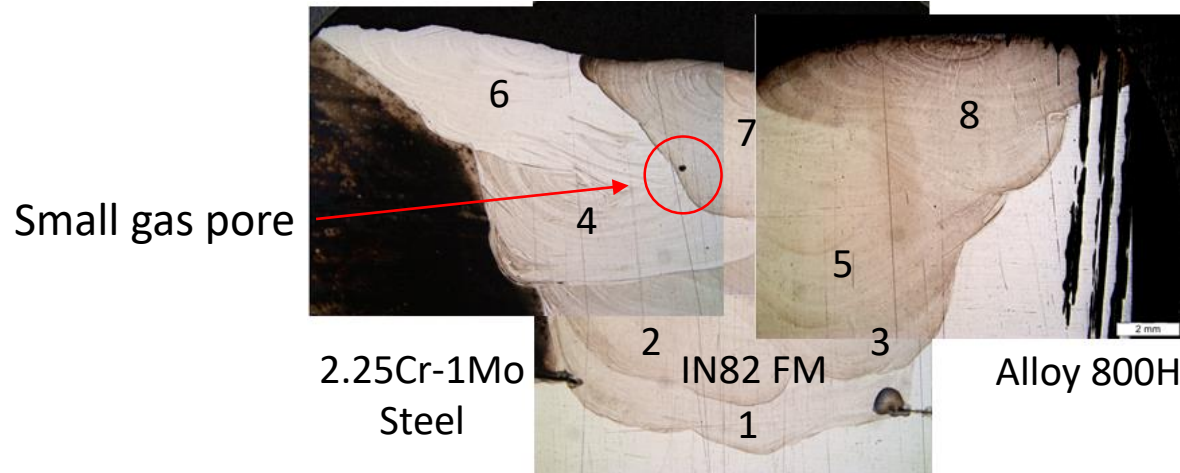
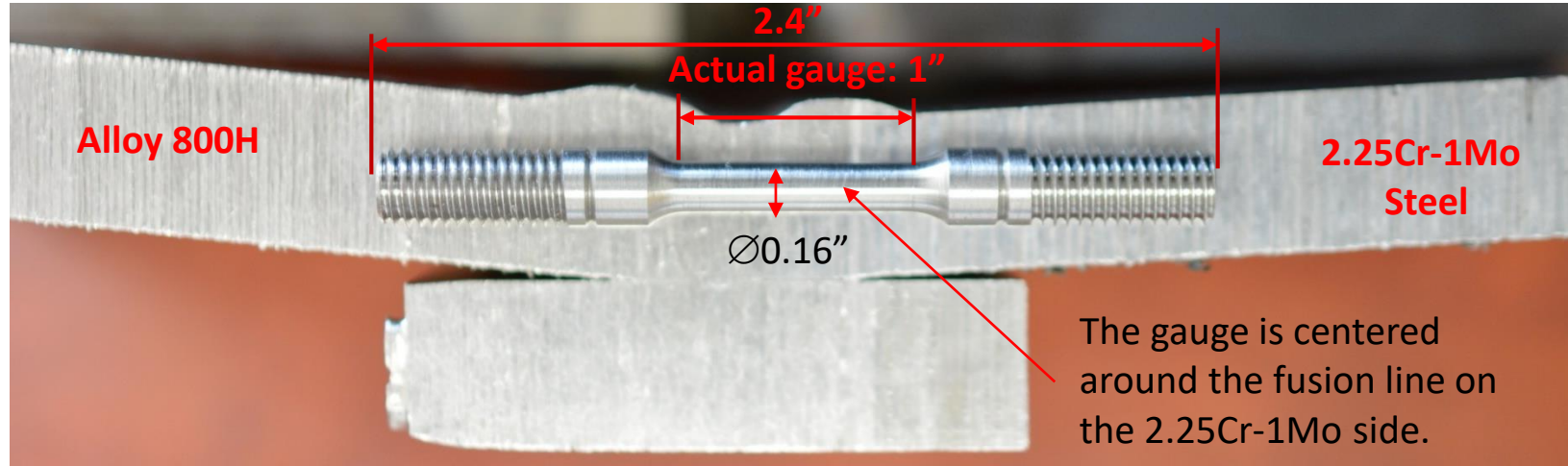


Temperature fields
Velocity distributions
Pool geometry



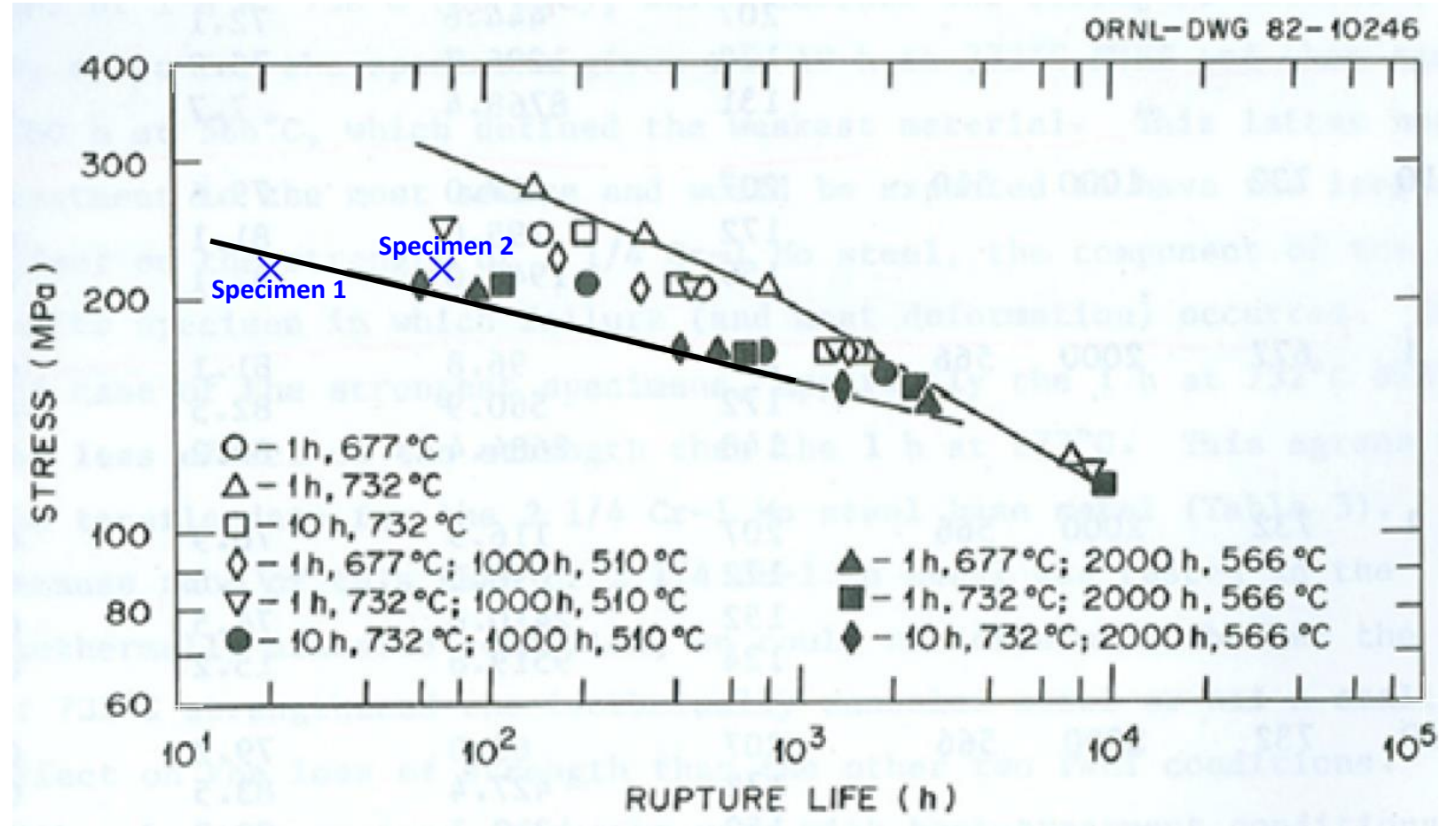
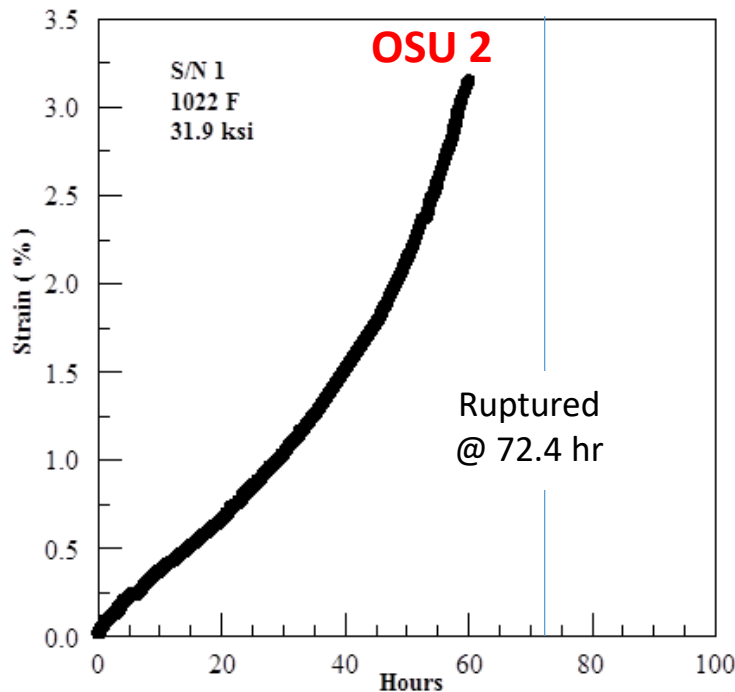
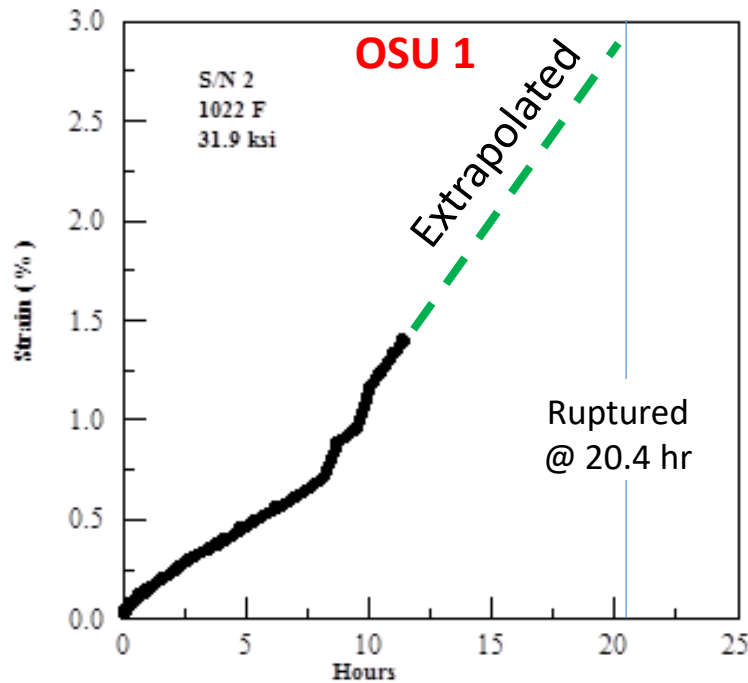
Gas Metal Arc Welding (GMAW):

- Average voltage: 21V
- Average current: 210A
- Wire feed speed: 300 ipm
- Travel speed: 10 ipm
- Electrode stick out: 1.5 cm
- Weaving amplitude: 3 mm
- Drag angle: 5 deg.
- Preheat temperature: 280 °C
- Filler metal: FM 82
- Backing plate: Alloy 800H
- Shielding gas: Mixture of CO₂ and Ar



Creep Testing at 220 MPa and 550°C

Baseline creep data agrees well with previous literature



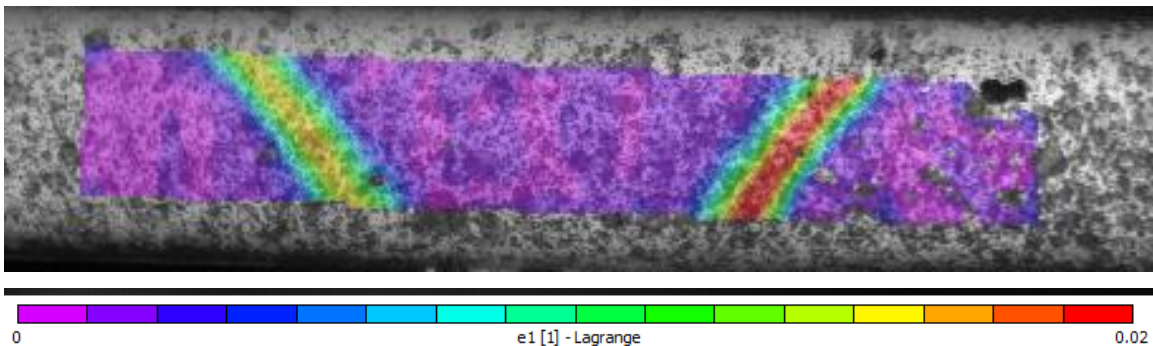
Klueh, K. L. and King, J. F. *Elevated temperature Tensile and Creep-Rupture Behavior of Alloy 800H/ERNiCr-3 Weld Metal/2.25Cr-1Mo Steel Dissimilar-Metal Weldments.* (ORNL, 1982)

Specialized Creep Testing

- Due to the inhomogeneity of the graded transition joints, traditional creep testing will not capture the creep behavior sufficiently
- Specialized creep testing using digital image correlation will show localized strain rates

Step 1: Dissimilar metal weld

- Test weld with same process and creep test parameters used at OSU
- Compare results with baseline data to validate the method
- Identify regions of localized strain



Creep strain map of a Grade 91 cross-weld sample showing localized deformation

Step 2: Graded transition joint

- Test a graded transition joint fabricated at PSU using the in house DED-AM machine
- Compare results with baseline data to see anticipated improvement in creep performance
- Identify regions of localized strain



SS316/T22 DMW sample image after 378 hours creep testing

Acknowledgements



PennState

MatSE

MATERIALS SCIENCE AND ENGINEERING

COLLEGE OF EARTH AND MINERAL SCIENCES



Nuclear Energy University Programs

